SiMRTRANS

Simulation of an Anti-Lock Braking System in a MATLAB/Simulink Environment for Various Road Adhesion Properties

Łukasz KACPRZYCKI, Mateusz BRUKALSKI*,
Michał Mariusz ABRAMOWSKI, Hubert SAR, Piotr FUNDOWICZ

Institute of Vehicles and Construction Machinery Engineering
Warsaw University of Technology
Warsaw, Poland; e-mails: michal.abramowski@pw.edu.pl, hubert.sar@pw.edu.pl,
piotr.fundowicz@pw.edu.pl

*Corresponding Author e-mail: mateusz.brukalski@pw.edu.pl

Driving safety is very important to every vehicle user. Automobile manufacturers compete by introducing increasingly advanced safety systems, which, when combined with appropriate driver response, help prevent road accidents. The demand for such systems in vehicles has been driven mainly by the dynamic development of automotive industry and continually increasing number of vehicles on the road. This paper deals with safety systems that monitor wheel longitudinal slip, with emphasis on testing an anti-lock braking system (ABS) in a MATLAB/Simulink environment. The aim of the work is to describe the development and operation of ABS, electronic stability program (ESP), acceleration slip regulation (ASR) and electronic brakeforce distribution (EBD) systems, and to develop a simulation model of ABS. The relationship between the tire-to-road adhesion coefficient and longitudinal wheel slip was modeled using the Magic Formula equation. The contribution of this system to the vehicle's braking process on various surfaces (dry asphalt, wet asphalt, snow, and ice) and at various initial velocities was analyzed. In particular, braking distance as a function of time comparing scenarios with ABS activated and deactivated is presented. The structure of the paper includes a theoretical part overviewing automotive safety systems, a description of the ABS model, and an analysis of the results.

Keywords: automotive safety systems; ABS; ESP; ASR; EBD; active safety systems; Magic Formula.

1. Introduction

Safety plays a very important role when traveling by car. Therefore, great attention is paid to developing safety systems based on wheel slip monitoring, such as ABS, ESP, ASR, and EBD. Engineers are currently focusing on devel-

oping the safety systems used in vehicles, and manufacturers are competing in the market by introducing newer ideas and innovative solutions.

Systems such as ABS, ESP, ASR, and EBD have become essential elements of modern cars. Additionally, manufacturers offer a number of other safety solutions, competing in terms of their innovation Examples include: brake assist system (BAS), which supports the driver during emergency braking, or blind spot information system (BLIS), which detects vehicles in the blind spots. The automatic braking system is another helpful feature, applying the brakes automatically instead of driver in an emergency situation.

Electronic security systems belong to the so-called active safety, which includes elements of a car's equipment and structure designed to reduce the likelihood of collisions and road accidents. However, it is important to remember that active safety is not just about electronics. Much also depends on the driver's skills, reaction time, and decisions made in a threatening situation. Active safety is also influenced by the driver's overall condition, including fatigue, awareness, and sobriety. Various scientific sources explore the impact of driver properties, such as reaction time, on safety [1–5]. For example, a driver's drowsiness can be extremely dangerous, particularly during braking, even if the vehicle is equipped with ABS or any other automotive safety solutions. The issue of driver drowsiness is mentioned in [6, 7]. Additionally, the condition of the vehicle plays an important role, including factors such as its brakes, tires and general technical condition [8].

It is justified to conduct researches on active safety systems in vehicles to sustain their continuous development. One example is the study presented in [9], where the authors highlight problems with the functioning of the ABS system resulting from highly nonlinear dynamics and some uncertainties regarding parameters in its dynamics. The authors of [9] present their findings in support of a special ABS test rig with a custom controller. Another study on the ABS is presented in [10], where the authors explain the role of a fuzzy controller of ABS system in improving the properties of the braking process, in particular its performance on wet road surfaces. The article [8] examines the influence of vehicle velocity, tire age, and ABS on tire-to-road adhesion coefficient and braking distance. The research compares scenarios with the ABS activated and deactivated on both wet and dry road surfaces. The research also considers different initial braking velocities.

In [11], the authors present the application of online model predictive control for the ABS to maintain the tire-to-road adhesion coefficient close its maximum, known as the peak adhesion coefficient. The study also discusses the functioning of ABS under different adhesion conditions. A quarter-car model is used in [11], which follows a similar approach to the one in our paper. In [12], the authors explore the cooperation between regenerative braking and ABS through the

application of explicit model predictive control (eMPC-CCS). Additionally, [12] presents the results of simulations of the braking process under varying adhesion coefficients, also including differences in adhesion between the left and right wheels.

In [13], it is stated that there is the possibility of adjusting the wheel slip tracking reference in order to maximize the braking forces under varying road conditions. These changing adhesion conditions are used to simulate dry asphalt, wet cobblestones, and snowy road surfaces. The approach is similar to our work, as the authors based their discussion on a quarter-car model.

In [14], there is presented a strategy to maximize energy recovery while maintaining safe braking maneuvers, including scenarios with μ-split road surfaces. On the right side, the adhesion coefficient was assumed to be 0.9, whereas in the case of the left path, it was set to 0.3. In [15], the authors explore how to recognize road surface conditions with the application of on-board sensors in a vehicle equipped with active safety systems. One of the aims of this study was to predict the optimal range of longitudinal slip changes based on different conditions of tire-to-road surface adhesion properties. The work in [16] presents a concept for shortening braking distance and enhancing recuperated energy using fuzzy logic control (FLC). The challenge of finding the optimal range of longitudinal slip ratio between the tire and road, which results in peak (maximum) adhesion coefficient is also discussed in [16].

In [17], the authors discuss the information concerning the cooperation between in-wheel electric motors and an electro-hydraulic ABS through a slip control algorithm. Seeking the optimal value of the longitudinal slip ratio is one of the main objectives of the article [17], which also examines adhesion characteristics under various adhesion conditions. Similarly to [17, 18] presents a comprehensive analysis of electric brakes and conventional friction brakes in electric-driven vehicles.

Emergency braking has impact on the frame of the truck tractor, as examined [19]. The authors discuss the effects of the tractor frame under sudden vehicle deceleration, including, among others, factors such as the tire-to-road adhesion coefficient, simulating dry asphalt-concrete road pavement. In paper [20], the authors present an analysis of vehicle motion with the application of a twelve-degree-of-freedom model of a vehicle to assess its motion stability. Additionally, a simple interpretation of driver behavior, as well as steering system stiffness, is presented. The tribological properties of the brake disc – brake pad pair influence the braking process of an automobile. Paper [21] shows the results of investigations into the properties of materials used for semi-metallic brake pads, with a particular focus of wear mechanisms.

The review of literature presented above shows the importance of investigating the braking process, particularly in relation to the ABS. Many of the

studies discussed consider varying tire-to-road adhesion conditions as the relationships between adhesion coefficient and slip ratio (both in the longitudinal direction). The materials used in the tribological pairs of braking mechanisms also play a significant role, especially during sudden, extreme braking, where high temperature gradients occur in these components.

2. Simulation model of the ABS system controller

This work presents a model of the ABS system and its impact on braking distance. Based on the built model, simulation tests were carried out, taking into account various initial velocities and road surfaces, including dry asphalt, wet asphalt, snow, and ice. For this purpose, a model was created in the MATLAB Simulink [22] program, which accounts for the physical processes occurring during vehicle braking. The tests were carried out at velocities of 10 m/s (36 km/h), 20 m/s (72 km/h), 30 m/s (108 km/h), and 40 m/s (144 km/h).

The Simulink program was used for the research, as it is a platform for multi-domain simulation and design of dynamic systems using models. It provides an interactive graphical environment and a collection of libraries of configurable blocks. This enables precise design, simulation, and implementation. It also enables integration with other systems defined in the time domain.

2.1. Initial parameters

The car used for the simulation was a Toyota Yaris. The car parameters used in the simulation are presented in the table below (Table 1).

Table 1. Technical data of the Toyota Yaris [23].

Parameter	Values
Mass per wheel m	385 kg
Tire size	185/60R15
Wheel dynamic radius r_d	0.2925 m
Moment of inertia of the driving wheel I_k	0.7 kgm^2

The following parameters were included in the simulation tests:
- Mass per wheel (quarter of the car) – this value reflects the mass that affects the inertia of the system and braking force,
- Gravitational acceleration – determined based on geographical location ($g = 9.81$ m/s^2),
- Dynamic radius – the radius that changes as the vehicle moves,

- Moment of inertia of a wheel – a value determined on the basis of the mass distribution of the wheel and rim relative to the axis of rotation of a wheel. It depends on the type of tire and the design of the selected rim,
- Initial velocity – this is a very important parameter for the entire project and was varied during the subsequent simulation tests in order to check is impact on wheel slip during braking, as well as on braking time and distance,
- Type of road surface – the last parameter of the simulation, which was also altered and taken into account during the simulation tests, considers the impact of driving with and without ABS on slippery surfaces such as ice or snow. To simulate this, appropriate values should be entered into their corresponding block (1 – dry asphalt, 2 – wet asphalt, 3 – snow, 4 – ice).

2.2. Initial parameters

The main task of the ABS system during vehicle braking is to maintain an appropriate wheel slip, which is defined as the quotient of the difference between the translational velocity of the wheel center and the theoretical circumferential velocity of the wheel divided by the translational velocity of the wheel center during braking. The highest coefficient of longitudinal adhesion between the tire and the surface on which a car is moving occurs for slip values of approximately 0.2 for dry asphalt, 0.09 for wet asphalt, 0.25 for snow, and 0.4 for ice. By maintaining the highest possible longitudinal adhesion coefficient, the vehicle does not lose steerability, as confirmed by the analysis of the simulation test results.

$$(2.1) \qquad \lambda = \frac{v_k - \omega_k \cdot r_d}{v_k},$$

where λ – longitudinal wheel slip, v_k – forward velocity of the wheel center, ω_k – angular velocity of the wheel, and r_d – dynamic radius of the wheel.

2.3. Magic Formula – cooperation between the wheel and the road surface

The Magic Formula is an equation that determines the braking force based on wheel slip and the vertical load of the vehicle. The inputs to the equation include wheel slip, vertical load. and five coefficients characteristic of the given surface. Table 2 presents the coefficients for different surfaces on which the vehicle is driving.

The Magic Formula [25] is a specific form of a tire's characteristic function, characterized by four dimensionless coefficients B, C, D, and E, i.e., stiffness, shape, peak and curvature, respectively. The Magic Formula equation is often

TABLE 2. Magic Formula parameter table [24].

Road surface	B	C	D	E
Dry asphalt	10	1.9	1	0.97
Wet asphalt	12	2.3	0.82	1
Snow	5	2	0.3	1
Ice	4	2	0.1	1

mentioned and applied in many studies, such as [9, 12, 14, 16, 20] already cited in the first section of this article. The equation [25] is presented below:

$$(2.2) \qquad F_x = F_z \cdot D \cdot \sin\Big(C \cdot \arctan\Big(B \cdot \lambda - E \cdot \big(B \cdot \lambda - \arctan(B \cdot \lambda)\big)\Big)\Big),$$

where F_x – brake force [N], F_Z – vertical load [N], λ – wheel slip [–], and B, C, D, E – coefficients depending on the surface on which the vehicle is driving.

Figure 1 shows the course of the longitudinal adhesion coefficient between the tire and the road surface as a function of wheel slip. The figure shows the courses for four different surfaces that were analyzed. The highest longitudinal adhesion coefficient was achieved for dry asphalt and a slip of 0.2. As observed in the graph, the course of the longitudinal adhesion coefficient varies for different surfaces, showing non-proportional relationships and different shapes. This variation may have a significant impact the results in the subsequent simulation study. In order to create the graph, the appropriate coefficients were defined in the MATLAB program, and a function was created to calculate the longitudinal adhesion coefficient as a function of slip.
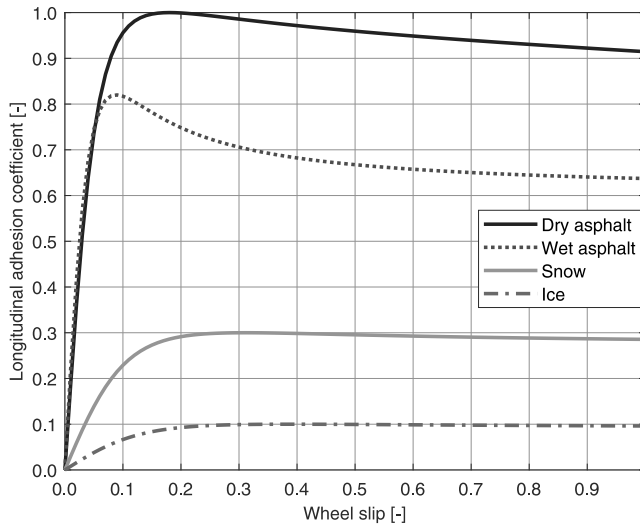

FIG. 1. Graphs of the longitudinal adhesion coefficient for given surfaces (Magic Formula [25]).

If both sides of Eq. (2.2) [25] are divided by the vertical load, we obtain an equation that results in the longitudinal adhesion coefficient:

$$(2.3) \qquad \frac{F_x}{F_Z} = D \cdot \sin\left(C \cdot \arctan\left\{B \cdot \lambda - E\left[B \cdot \lambda - \arctan(B \cdot \lambda)\right]\right\}\right) = \mu_w,$$

where μ_w is the longitudinal adhesion coefficient.

This equation was modeled using blocks in the MATLAB Simulink environment, as can be seen in Fig. 9. The input values to the equation are the longitudinal slip λ and the coefficients B, C, D, and E, which are responsible for mapping the slip for a given road surface. The output value is the coefficient of longitudinal adhesion of the tire to the road surface.

2.4. Calculating braking distance

Based on the calculation of the longitudinal adhesion coefficient, the longitudinal road reaction F_x occurring between the wheel and the surface was calculated:

$$(2.4) \qquad F_x = mg\mu_w.$$

This value was then multiplied by the dynamic radius of the wheel r_d, and the torque M_x resulting from this reaction was obtained:

$$(2.5) \qquad M_x = F_x r_d.$$

On the basis of the moment coming from the longitudinal reaction of the road divided by the mass per wheel, the linear acceleration of the vehicle was obtained. This value should be multiplied by -1 due to the direction of the force. In this way, the deceleration a_b is obtained:

$$(2.6) \qquad a_b = -\frac{M_x}{m}.$$

By integrating the vehicle braking deceleration, the velocity V_k of the wheel center is obtained:

$$(2.7) \qquad V_k(t) = \int_0^{t_b} a_b \, \mathrm{d}t + C_1 = a_b t_b + C_1,$$

where C_1 is the value of the integration constant, and t_b is the braking time.

It was assumed that $V_k(0) = V_0$. So $C_1 = V_0$. The relationship describing the velocity of the wheel center takes then the following form:

$$(2.8) \qquad V_k(t_b) = V_0 + a_b t_b.$$

By integrating the forward velocity of the wheel center V_k, the braking distance s_b was obtained:

$$(2.9) \qquad s_b(t) = \int_0^{t_b} V_k \, \mathrm{d}t + C_2 = \int_0^{t_b} (V_0 + a_b t_b) \, \mathrm{d}t + C_2,$$

where C_2 is the value of the integration constant.

It was assumed that $s_h(0) = 0$. So $C_2 = 0$. The relationship describing the vehicle's braking distance s_b is as follows:

$$(2.10) \qquad s_b(t_b) = V_0 t_b + \frac{1}{2} a_b t_b^2.$$

2.5. Dynamics of the braking system including the ABS system

Based on the information about the values of the longitudinal slip λ and the desired slip, the error of the desired slip is calculated. In order to examine the influence of the surface on ABS operation, the desired slip value was set to 0.2 for all analyzed surfaces. Due to the specific operation of the ABS system, braking with the maximum possible force, the control strategy was designed as a two-state controller (-1 for no braking and 1 for maximum braking force).

In order to make the simulation tests as realistic as possible, a first-order transfer function block, representing the deceleration dynamics of the braking system, was added. This transfer function $G(s)$ is expressed by:

$$(2.11) \qquad G(s) = \frac{6000}{0.0001s + 1}.$$

Without this block, the system's response would be immediate and the desired slip would be adjusted almost instantaneously. In the next step, this output signal is integrated, but with an upper integration limit imposed to represent the maximum braking torque. This limit is set to 1500 Nm. The last step in this part of the model is to calculate the error between the torque that can be transmitted by the wheel and the torque generated by the vehicle's friction brakes. This difference is further used in the ABS control algorithm.

2.6. Calculation of the angular velocity of the wheel

The wheel's angular velocity ω_k was calculated on the basis of the torque error ΔM_b resulting from the difference between the torque generated by the longitudinal road reaction and the braking torque applied by the braking system:

$$(2.12) \qquad \Delta M_b = M_x - M_b,$$

where M_x – the torque resulting from the longitudinal road reaction, and M_b – the braking torque generated by the operation of the braking system.

The obtained moment ΔM_b was divided by the moment of inertia of the wheel I_k in order to obtain the angular acceleration ε_k:

$$(2.13) \qquad \varepsilon_k = \frac{\Delta M_b}{I_k}.$$

By integrating the angular acceleration of the wheel, the angular velocity ω_k was obtained:

$$(2.14) \qquad \omega_k(t) = \int_0^{t_b} \varepsilon_k \, \mathrm{d}t + C_3,$$

where C_3 is the value of the integration constant.

It was assumed that $\omega_k(0) = \omega_0$. Therefore, $C_3 = \omega_0 = V_0/r_d$. The relationship describing the angular velocity of the braked wheel ω_k is as follows:

$$(2.15) \qquad \omega_k(t_b) = \varepsilon_k t_b + \frac{V_0}{r_d}.$$

Due to the calculation method used, a logical condition was implemented to check whether the vehicle's wheel is locked. This condition corrects any negative angular velocity values that may arise during the computation.

3. Simulation studies

Based on the simulation model built in MATLAB Simulink, the influence of the type of surface, initial velocity and operation of the ABS system on the length of the braking distance was analyzed. In the first part, the influence of initial velocity on the braking distance was examined for both inactive and active ABS systems. In the second stage, the influence of the type of surface on braking distance was analyzed with the ABS system both turned off and on, for different initial braking velocities. To improve clarity, the braking distance results are presented in the form of line graphs and bar charts. Additionally, the average braking deceleration was calculated for each type of surface (with ABS turned off and on), and these results are also presented as bar charts.

3.1. Analysis of braking distance for different initial vehicle velocities

In the first stage of the simulation tests, braking distance values for a vehicle with known and given parameters were compared. During multiple simulations, the results were obtained for each type of surface:

- dry asphalt,
- wet asphalt,
- snow,
- ice.

For each surface type, tests were carried out taking into account four initial vehicle velocities:

- 10 m/s,
- 20 m/s,
- 30 m/s,
- 40 m/s.

Additionally, the influence of ABS system was examined by conducting each test under two conditions:

- ABS activated,
- ABS deactivated.

Based on these simulations, the charts were presented showing the test results for a specific surface along with information about the ABS system turned on or off. The number of variables in simulation tests allows to 32 independent vehicle braking distances. The simulation results were divided into eight graphs. Each graph presents braking distances over time for specific road conditions and for a vehicle without ABS or equipped with it.

As can be seen in the graph below (Fig. 2), the braking distance does not change linearly with higher velocity. The curve responsible for the braking dis-
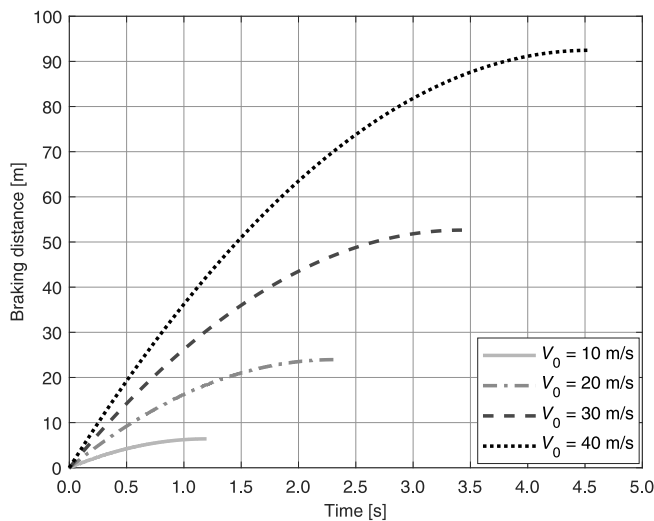
FIG. 2. Braking distance for the simulation (dry asphalt, no ABS).

tance s_b as a function of the vehicle's initial velocity can be determined from the following formula:

$$(3.1) \qquad s_b = \frac{V_0^2}{2\mu_w g},$$

where s_b – braking distance [m], V_0 – initial velocity of the vehicle [m/s], μ_w – longitudinal adhesion coefficient, and g – gravitational acceleration [m/s^2].

This formula shows that the braking distance is proportional to the square of the vehicle's velocity and depends on the vehicle's deceleration during braking. The deceleration depends mainly on braking conditions, with its maximum value being the product of gravitational acceleration due and the longitudinal adhesion coefficient. The formula also shows that the braking distance does not depend on the vehicle's weight; however, the longitudinal adhesion coefficient partially depends on the vertical load. Additionally, incorrect weight distribution in the vehicle leads to uneven pressure distribution of the wheels, which affects braking efficiency. Moreover, improper adjustment or ineffective operation of the braking system leads to an in-appropriate distribution of braking forces across individual wheels.

Based on the analysis of the figures for braking on a dry asphalt surface with the ABS system turned off (Fig. 2) and with the ABS system turned on (Fig. 3), the difference in braking distance at the lowest tested initial velocity is small. However, at the highest tested initial velocity, the difference in braking distance is almost 6 meters. This system ensures vehicle steerability, which,
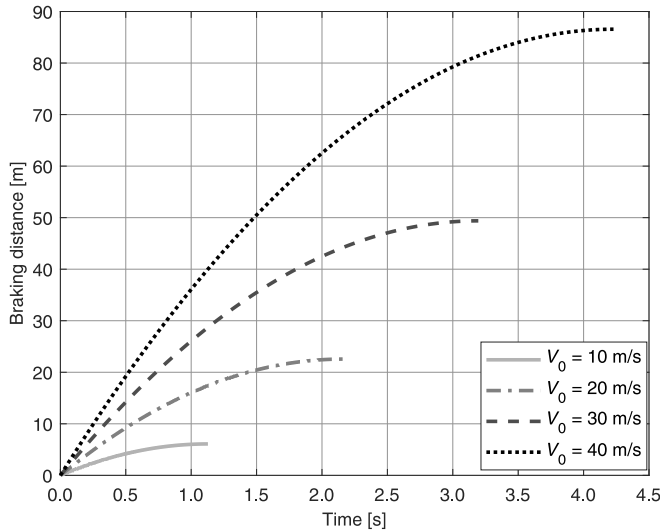
FIG. 3. Braking distance for the simulation (dry asphalt, ABS).

over a distance of over 85 meters, could translate into the ability to avoid an obstacle and prevent a car accident.

In order to achieve the best grip during braking, the desired slip value between the vehicle and its wheel was adjusted to 0.2, which resulted in the longitudinal adhesion coefficient reaching a value in the range of 0.8 to1.

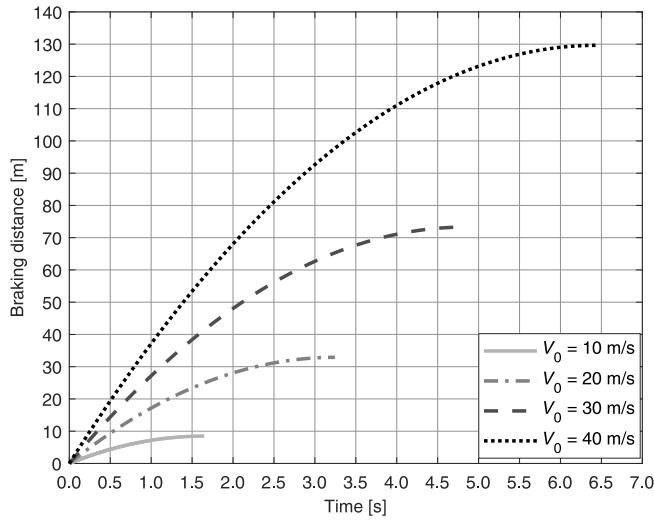Comparing the braking distance charts for a wet asphalt surface, both with the ABS system deactivated (Fig. 4) and with the ABS system activated (Fig. 5),

FIG. 4. Braking distance for the simulation (wet asphalt, no ABS).
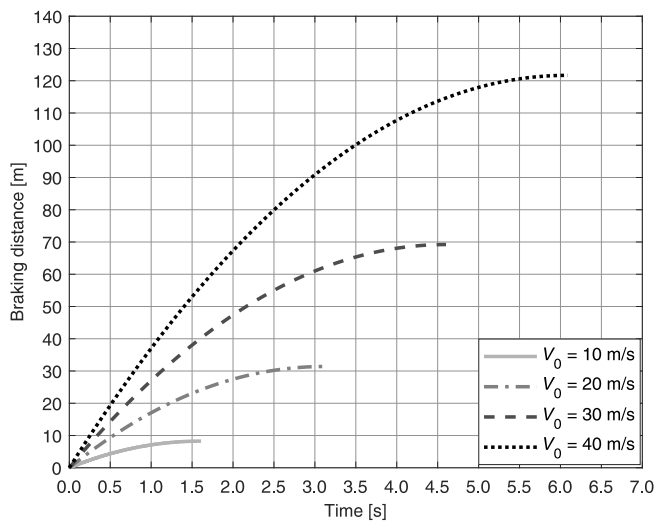
FIG. 5. Braking distance for the simulation (wet asphalt, ABS).

it can be concluded that the braking distance at an initial velocity of 40 m/s was shortened by approximately 8 meters. This proves the influence of the ABS system on maintaining grip between the tire and the road surface. By analyzing the graph of the longitudinal adhesion coefficient as a function of wheel slip (Fig. 1), it can be seen that, especially for the parameters of the equation for wet asphalt, maintaining appropriate slip is important for shortening the braking distance.

The braking distance graph for snow (Fig. 6) shows that, compared to wet asphalt (Fig. 5), the braking distance is twice as long. This is the result of the reduction in the longitudinal adhesion coefficient.
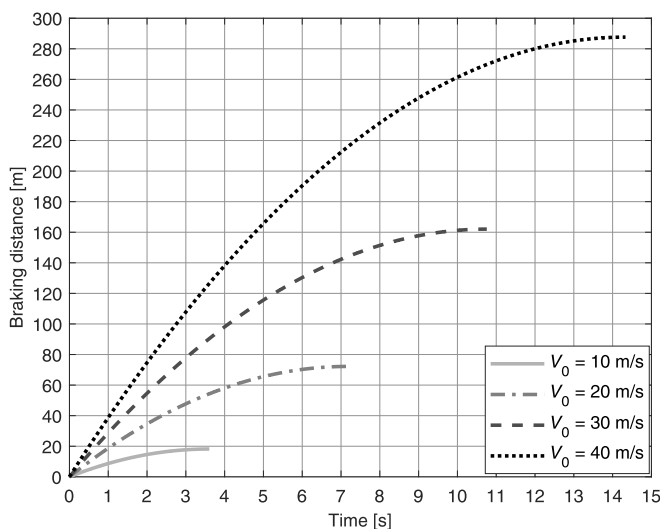
FIG. 6. Braking distance for the simulation (snow, no ABS).

Comparing the braking distance graph for snow, with and without the ABS system, it can be observed that at a velocity of 40 m/s (140 km/h), the braking distance is shortened by only a few meters. Taking into account the fact that in Poland, this speed is only permitted on highways – which are properly prepared for the winter season – this situation may not accurately reflect real-life conditions. However, when comparing a velocity of 30 m/s (108 km/h), we can observe a slight impact of the ABS system on the braking distance on snow-covered surfaces. Such weather conditions often accompany the winter season in Poland. However, the ABS system improves vehicle controllability, helping the driver avoid obstacles and minimizing consequences of an accident.

Analyzing the graph for a snow surface with the ABS system (Fig. 7), it can be noticed that even a velocity of 20 m/s results in a very long braking period, which is close to the value in the case of dry asphalt at highway velocity
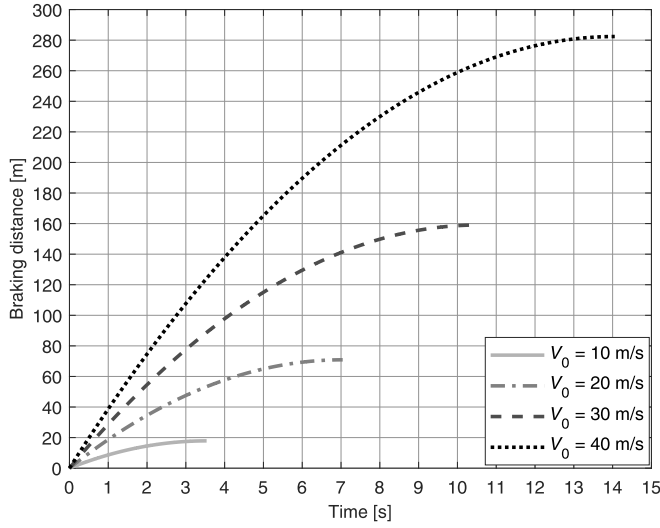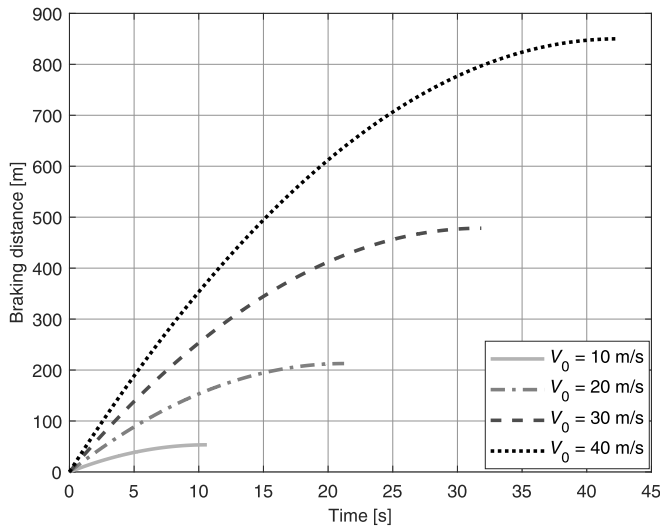
Fig. 7. Braking distance for the simulation (snow, ABS).

with the ABS system (Fig. 3). The time course of the braking distance for snow shows that even a low velocity can be very dangerous if the vehicle needs to be suddenly braked.

In the case of an icy surface, the longitudinal adhesion coefficient as a function of slip becomes approximately constant for slips greater than 0.2 (Fig. 1). Similarly to the snow surface, there is no significant difference in the braking distance of a vehicle with ABS (Fig. 9) or without ABS (Fig. 8).

Fig. 8. Braking distance for the simulation (ice, no ABS).
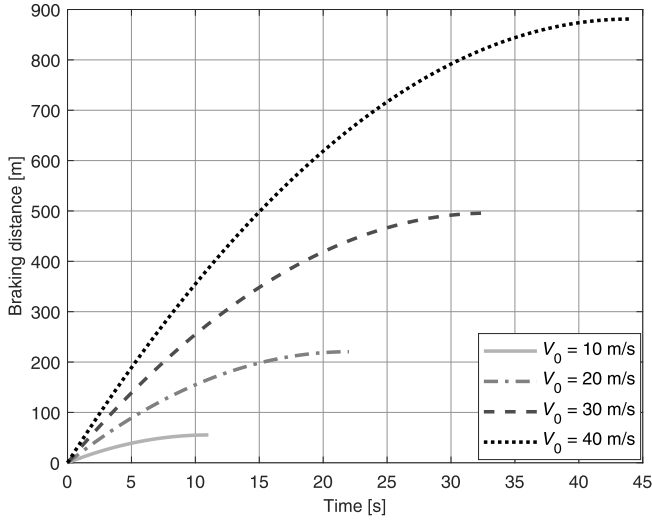
FIG. 9. Braking distance for the simulation (ice, ABS).

3.2. Braking distance analysis for various road surfaces

In this chapter, the braking distance results for different surfaces with the same initial velocity are compared. First, the results for braking without the ABS system are s presented, followed by the results with the ABS system on. In the following graphs, the initial velocity of the vehicle is increased (10 m/s, 20 m/s, 30 m/s, 40 m/s). The purpose of the graphs presented in this chapter is to show the influence of the road surface on the braking distance.

The first graph presented in this section (Fig. 10) shows that the distance covered by the car on dry and wet asphalt is very similar. Only the braking time differs in relation to the distance traveled. Unfortunately, the braking distance on snow is twice as long as the braking distance on dry asphalt, despite the low initial velocity. However, the biggest difference is between braking on ice and braking on other surfaces. The distance covered by the tested car at an initial velocity of 10 m/s is approximately 55 m.

Comparing the first graph (Fig. 10) with the next one (Fig. 11), there is no significant reduction in the braking distance compared to the simulation tests without the ABS system. Once again, it can be noticed that the distance needed to stop a vehicle moving on dry asphalt is much smaller than the braking distance of a vehicle moving on ice or snow.

Despite presenting many graphs in this work showing the distance traveled by the vehicle during braking and comparing the velocity or the surface on which the vehicle was travelling, in many cases, the scale does not allow for a clear indication of the difference in the distance traveled. For this reason, additional
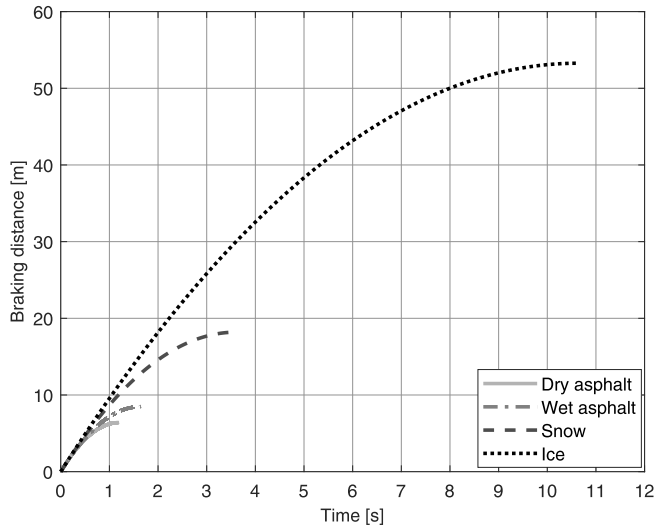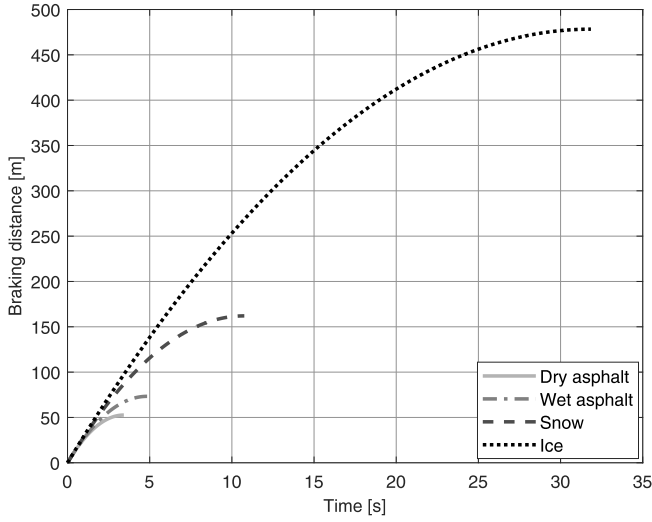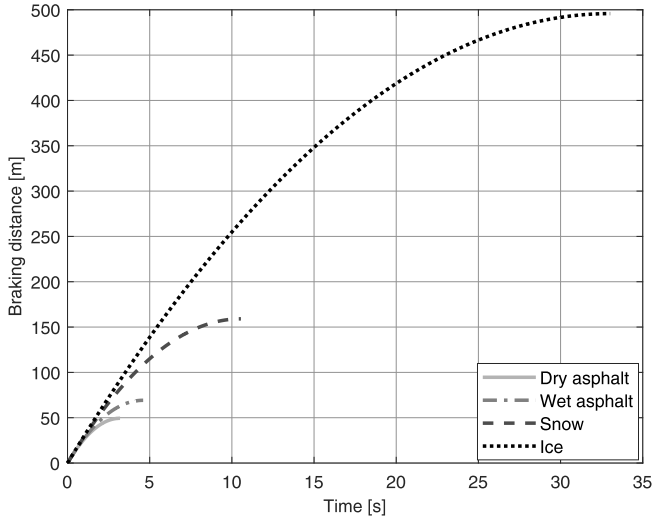
FIG. 10. Initial velocity $V_0 = 10$ m/s, no ABS.
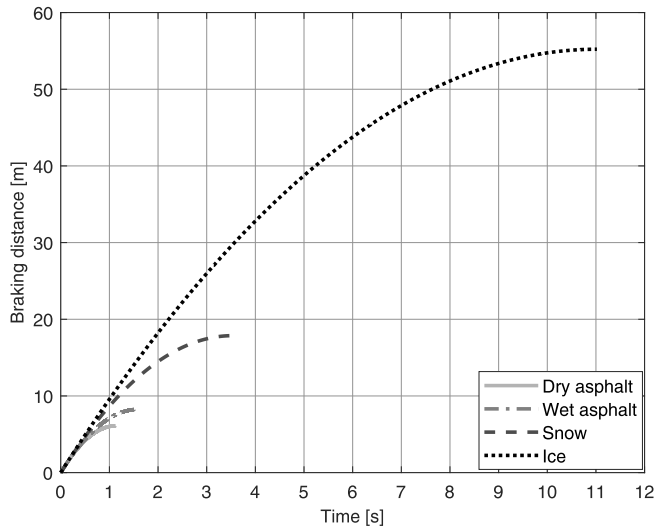
FIG. 11. Initial velocity $V_0 = 10$ m/s, ABS.

graphs showing the final braking distance for a given velocity have been added to our study. The results are divided into four graphs, each taking into account a different initial velocity of the vehicle.

The first figure (Fig. 18) shows the results for braking at an initial velocity of 10 m/s. The results of the braking distance without the ABS system engaged are marked in light gray, while the results with the ABS system engaged are
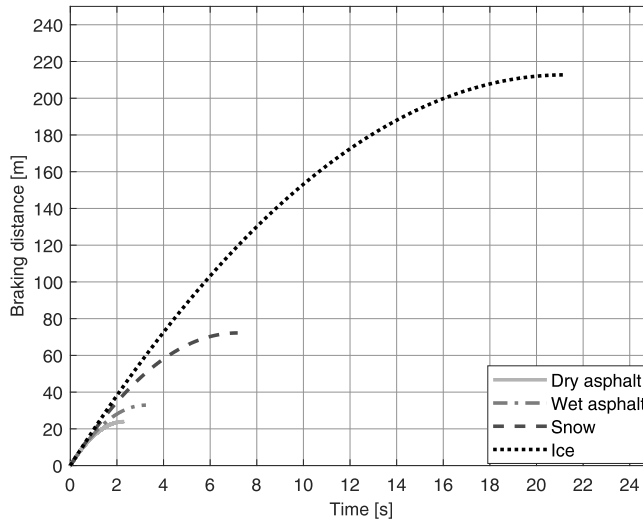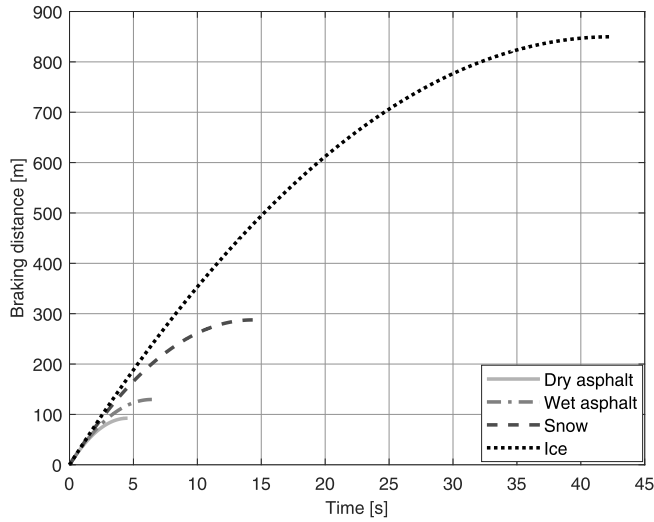
FIG. 12. Initial velocity $V_0 = 20$ m/s, no ABS.
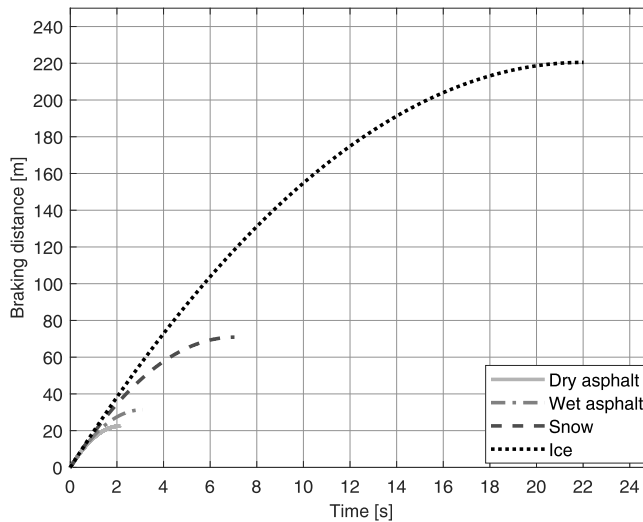
FIG. 13. Initial velocity $V_0 = 20$ m/s, ABS.

marked in dark gray. As can be observed in the graphs presented, the braking distances for dry asphalt and wet asphalt are similar. At each initial velocity tested, the ABS system shortened the braking distance on wet asphalt. This is very important because, to a large extent, when visibility is reduced due to rain, drivers may lose vigilance, which can lead to accidents. Unfortunately, on more "slippery" surfaces such as snow or ice, the braking distance increases when using the ABS system. It is worth noting, however, that there are also other

FIG. 14. Initial velocity $V_0 = 30$ m/s, no ABS.

FIG. 15. Initial velocity $V_0 = 30$ m/s, ABS.

systems in cars, which are not included in the simulation, that can contribute to improved safety. Thanks to the ABS system, on a 55 meters stretch of the road (ice, $V_0 = 10$ m/s), drivers are able to react and perform a maneuver to avoid pedestrians or obstacles, avoiding collisions or hitting bystanders.

The presented graphs also show that velocity is very important. For a velocity of 30 m/s, i.e., 108 km/h, the braking distance on an icy surface can be as long as 495 meters. This is a very long distance for urban agglomerations, and without

FIG. 16. Initial velocity $V_0 = 40$ m/s, no ABS.
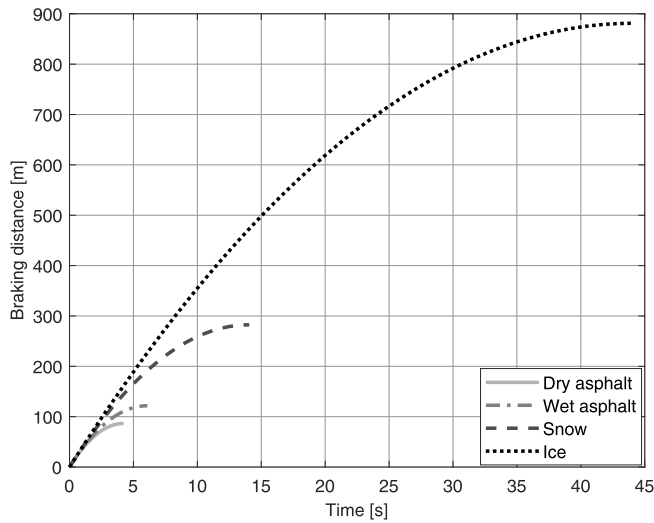
FIG. 17. Initial velocity $V_0 = 40$ m/s, ABS.

the mentioned system, a car could cause great destruction and pose a threat to people.

Analyzing the graphs comparing the braking distance for different initial velocity (Figs. 18–21), it can be seen that with the increase in the initial velocity, the braking distance increases for each type of surface on which the vehicle is moving. Regardless of the initial velocity, the shortest braking distance is achieved on dry asphalt, as it is characterized by the highest coefficient
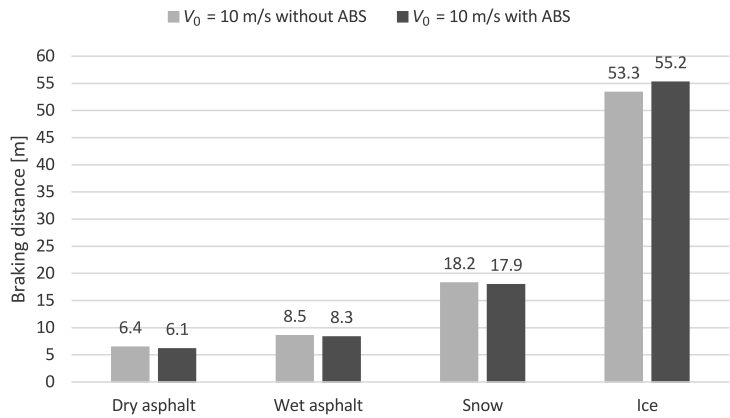
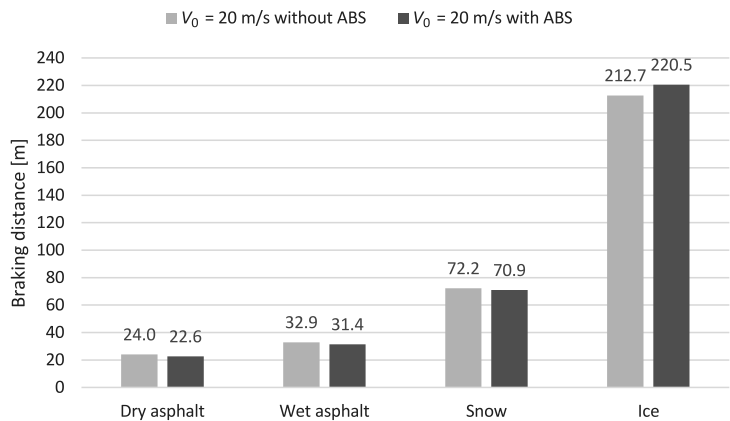FIG. 18. Graph comparing braking distance for $V_0 = 10$ m/s.

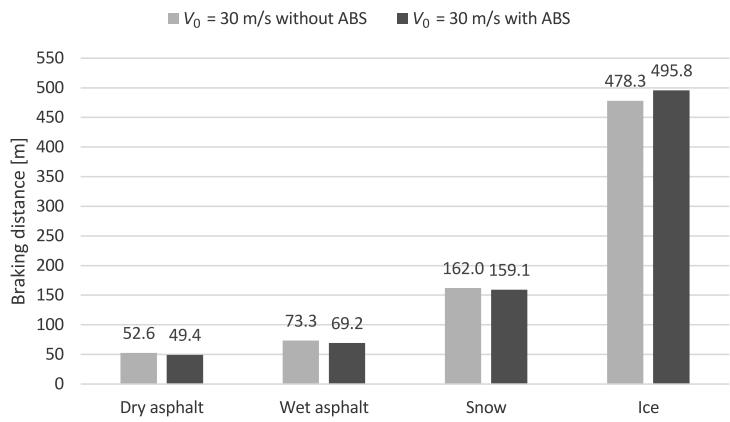FIG. 19. Graph comparing braking distance for $V_0 = 20$ m/s.

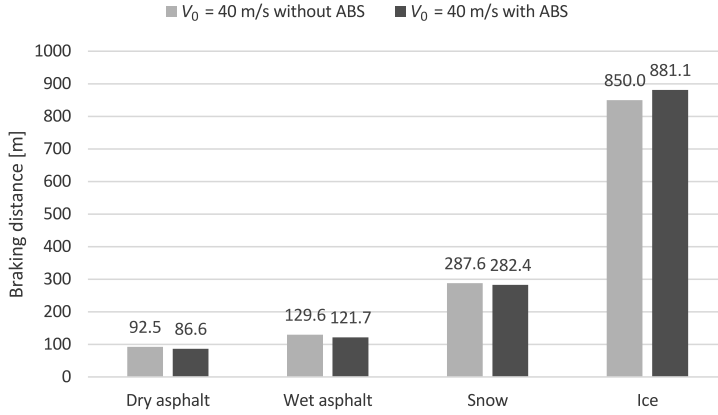FIG. 20. Graph comparing braking distance for $V_0 = 30$ m/s.

FIG. 21. Graph comparing braking distance for $V_0 = 40$ m/s.

of longitudinal adhesion. On the other hand, the longest braking distance occurs on an icy surface. The greatest difference in braking distance is observed between surfaces with the lowest and highest longitudinal adhesion coefficient. This difference, achieved for a vehicle moving at a velocity of 40 m/s, is nearly 800 meters. Regardless of the initial velocity, the ABS system for dry asphalt, wet asphalt and snow surfaces slightly shortens the braking distance, while in the case of icy surfaces the braking distance of a vehicle equipped with an ABS system is longer.

3.3. Braking distance analysis for various surfaces

The vehicle deceleration was calculated based on the formula below. The data needed for calculations are the initial velocity and the braking time, which was read from the braking distance charts. The charts present the absolute values of decelerations. Averaging the deceleration allows to show the differences that occur for the tested surfaces and the relationship between the results and the adhesion coefficient.

$$(3.2) \qquad a_b = \frac{\Delta V}{t_b} = \left| \frac{V_{\text{final}} - V_{\text{initial}}}{t_b} \right|,$$

where a_b – vehicle deceleration [m/s^2], V_{initial} –initial velocity of the vehicle [m/s], V_{final} – final velocity of the vehicle [m/s] for a stopped vehicle, $V_{\text{final}} = 0$ m/s, and t_b – braking time [s].

When analyzing the bar charts (Figs. 22–25), it can be noticed that regardless of the initial velocity, the vehicle's braking decelerations for individual surfaces are very similar to each other. The largest braking decelerations occur on the surface with the highest longitudinal adhesion coefficient, while the
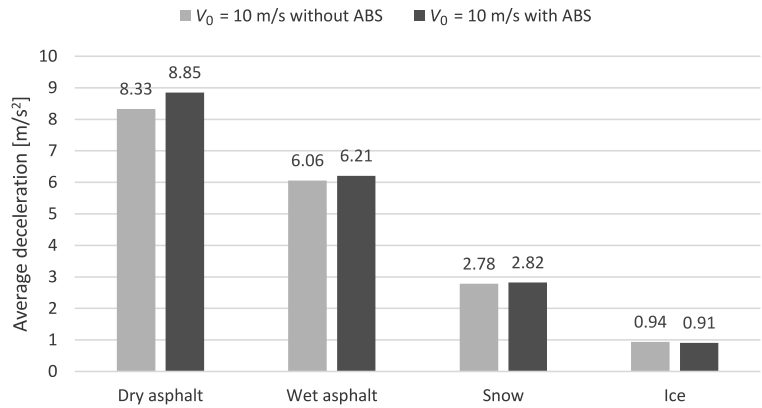
FIG. 22. Comparison of braking decelerations for initial velocity of 10 m/s.
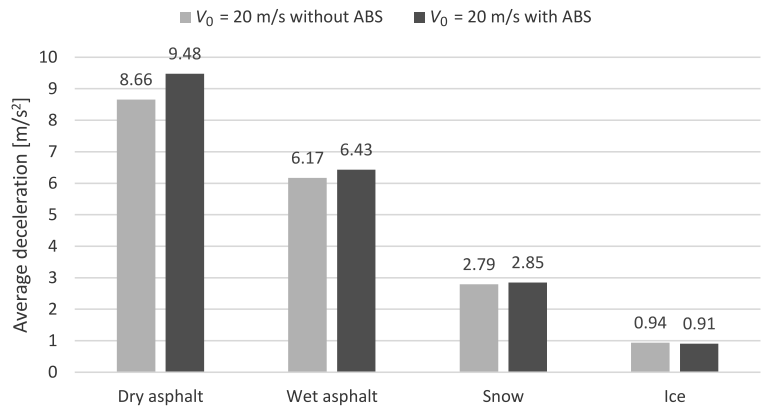

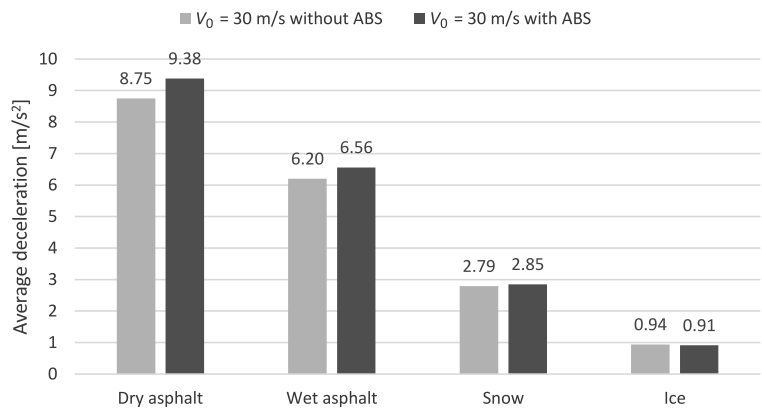FIG. 23. Comparison of braking decelerations for initial velocity of 20 m/s.

FIG. 24. Comparison of braking decelerations for initial velocity of 30 m/s.
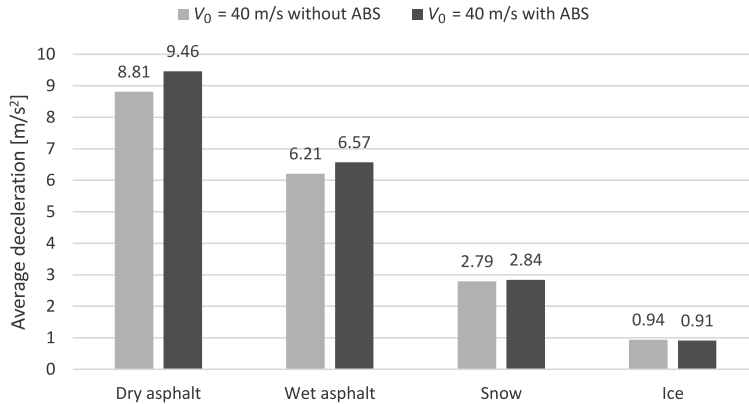
FIG. 25. Comparison of braking decelerations for an initial velocity of 40 m/s.

smallest are observed on the surface with the lowest longitudinal adhesion coefficient. For dry asphalt, wet asphalt and snow surfaces, a vehicle equipped with an ABS system achieves higher braking decelerations compared to a vehicle without such a system. In the case of icy surfaces, the ABS system slightly reduces the braking deceleration value.

3.4. The influence of the ABS system on wheel velocity

The ABS system allows the car to maintain directional stability by controlling the slippage of the braked wheels, preventing them from locking. Figures 26 and 27 show a comparison of the wheel center velocity and the wheel's circumferential velocity during a braking test with an initial vehicle velocity of 30 m/s
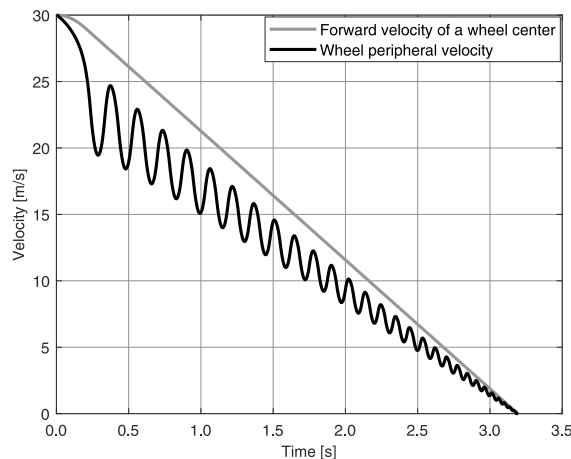

FIG. 26. Difference in the forward velocity of the wheel center and the wheel's circumferential velocity for dry asphalt with an initial velocity of 30 m/s with the ABS system active.
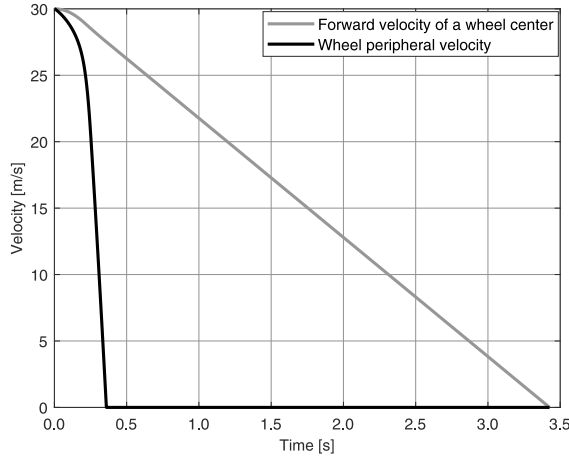
FIG. 27. Difference in the forward velocity of the wheel center and the circumferential velocity for dry asphalt with an initial velocity of 30 m/s with the ABS system turned off.

on a dry asphalt surface, both with the ABS system an active and inactive.

Figure 26 shows the situation during emergency braking of the vehicle, which shows that the driver presses the brake pedal with full force, yet the wheel does not lock. After a while, the ABS system is activated, detecting a large difference between the wheel and vehicle velocities. It then reduces the vehicle's braking force so that the slip is maintained at a set level. A given slip value of 0.2 allows for obtaining the highest longitudinal adhesion coefficient μ_w, which, in turn, provides a sufficiently high braking force on the vehicle's wheels to achieve the shortest braking distance.

The second graph presented in this chapter shows braking at the same initial velocity. In this case, the ABS system was not used, and the graph shows at which point the wheel was locked. Such a situation on the road causes the car to brake inertly for more than 3 seconds, moving forward, making it impossible to change the direction of travel.

4. SUMMARY AND FINAL CONCLUSIONS

Since the advent of automobiles, engineers and automotive manufacturers from all over the world aimed to improve safety systems to ensure that driving is a pure pleasure for the driver. Many manufacturers' main goal is to protect the health and life of travelers. Control algorithms related to the functioning of motor vehicles are constantly being developed, and security systems used in cars have also undergone significant evolution. Increasingly, the systems described in the introduction to this work interact with the driver's actions.

The equipment list of modern cars includes various systems designed to improve and ensure driving safety. Nowadays, practically every car comes with a range so-called "assistants" that support driving. These include: assistant for night driving, parking aids, lane-keeping systems, traffic jam navigation systems, and street traffic and road sign recognition systems. Of course, the number and types of systems available depend on the car model and make.

Safety systems in cars are very useful, but it should be remembered that they do not exempt drivers from driving carefully, observing their surroundings, and, above all, thinking and concentrating. This is because the dynamics of an automobile depend largely on the cooperation between the tire and the road surface. The situation becomes more complicated when tangential forces have to be transmitted at the contact patch between the tire and the road pavement not only in one direction, but in two. This means that if there is very intensive braking, there may not be enough capacity to transmit the lateral forces resulting from the car's curvilinear motion. This is one of the reasons why ABSs are used in vehicles, nowadays together with ESP. The final decision to perform any maneuvers on the road should always be made by the driver, who must be aware of potential dangers on the road, and avoid making hazardous maneuvers.

Based on the presented graphs, it can be concluded that due to the direct relationship between braking force and braking distance, breaking force has the greatest impact on the distance a vehicle must cover to stop. It is worth noting that braking distance does not depend linearly on the vehicle's initial velocity, so even a small difference in velocity can have a very tragic effect. When driving, for safety, it is important to follow road traffic regulations regarding the permissible and safe speed at which we can travel on public roads. The ABS system does not always shorten the braking distance [26]. Taking into account the ice surface, the braking distance is longer, while on the other three surfaces that were tested, the braking distance is shortened by several to over a dozen percent compared to a car without such a safety system. It should also be mentioned that this system provides increased traction and controllability of the vehicle, so despite the high initial velocity, the driving direction can still be changed, and braking can occur in a safe place. These few percentages provided by the ABS system may seem like a small value, but in the event of a collision with a pedestrian, who has much less mass compared to a car, it could save the pedestrian's life when they enter the road.

References

1. Jurecki R.S., Stańczyk T.L., Modelling driver's behaviour while avoiding obstacles, *Applied Sciences*, **13**(1): 616, 2023, https://doi.org/10.3390/app13010616.

2. Jurecki R.S., Stańczyk T.L., Jaśkiewicz M.J., Driver's reaction time in a simulated, complex road incident, *Transport*, **32**(1): 44–54, 2017, https://doi.org/10.3846/16484142.2014.913535.

3. Jurecki R.S., Jaśkiewicz M.J., Guzek M., Lozia Z., Zdanowicz P., Driver's reaction time under emergency braking a car – Research in a driving simulator, *Eksploatacja i Niezawodność – Maintenance and Reliability*, **14**(4): 295–301, 2012.

4. Ružić D., Bratić D., Nikolić N., Stojić B., Mačužić-Saveljić S., Investigation of a driver's reaction time and reading accuracy of speedometers on different instrument clusters of passenger cars, *Applied Sciences*, **15**(4): 1879, 2025, https://doi.org/10.3390/app15041879.

5. Lozia Z., Guzek M., System to assist the driver during a single lane change maneuver, in the conditions of danger arising from a change in the condition of the road surface, *Applied Sciences*, **14**(23): 11398, 2024, https://doi.org/10.3390/app142311398.

6. Choi Y., Yang S., Park Y., Choi C., Lee EC., Feasibility study on contactless feature analysis for early drowsiness detection in driving scenarios, *Electronics*, **14**(4): 662, 2025, https://doi.org/10.3390/electronics14040662.

7. Essahraui S., Lamaakal I., El Hamly I., Maleh Y., Ouahbi I., El Makkaoui K., Filali Bouami M., Pławiak P., Alfarraj O., Abd El-Latif AA., Real-time driver drowsiness detection using facial analysis and machine learning techniques, *Sensors*, **25**(3): 812, 2025, https://doi.org/10.3390/s25030812.

8. Lorenčič V., The effect of tire age and anti-lock braking system on the coefficient of friction and braking distance, *Sustainability*, **15**(8): 6945, 2023, https://doi.org/10.3390/su15086945.

9. García Torres C.J., Ferré Covantes L.A., Vaca García C.C., Estrada Gutiérrez J.C., Guzmán A.N., Acosta Lúa C., A Lyapunov stability analysis of modified HOSM controllers using a PID-Sliding surface applied to an ABS laboratory setup, *Applied Sciences*, **12**(8): 3796, 2022, https://doi.org/10.3390/app12083796.

10. Girovský P., Žilková J., Kaňuch J., Optimization of vehicle braking distance using a fuzzy controller, *Energies*, **13**(11): 3022, 2020, https://doi.org/10.3390/en13113022.

11. Seyyed Esmaeili J., Başçi A., Farnam A., Design and verification of offline robust model predictive controller for wheel slip control in ABS brakes, *Machines*, **11**(8): 803, 2023, https://doi.org/10.3390/machines11080803.

12. Chu L., Li J., Guo Z., Jiang Z., Li S., Du W., Wang Y., Guo C., RBS and ABS coordinated control strategy based on explicit model predictive control, *Sensors*, **24**(10): 3076, 2024, https://doi.org/10.3390/s24103076.

13. Meléndez-Useros M., Jiménez-Salas M., Viadero-Monasterio F., Boada B.L., Tire slip H∞ control for optimal braking depending on road condition, *Sensors*, **23**(3): 1417, 2023, https://doi.org/10.3390/s23031417.

14. Lv L., Wang J., Long J., Interval type-2 fuzzy logic anti-lock braking control for electric vehicles under complex road conditions, *Sustainability*, **13**(20): 11531, 2021, https://doi.org/10.3390/su132011531.

15. Castillo Aguilar J.J., Cabrera Carrillo J.A., Guerra Fernández A.J., Carabias Acosta E., Robust road condition detection system using in-vehicle standard sensors, *Sensors*, **15**(12): 32056–32078, 2015, https://doi.org/10.3390/s151229908.

16. Guo J., Jian X., Lin G., Performance evaluation of an anti-lock braking system for electric vehicles with a fuzzy sliding mode controller, *Energies*, **7**(10): 6459–6476, 2014, https://doi.org/10.3390/en7106459.

17. Ko S., Song C., Park J., Ko J., Yang I., Kim H., Comparison of braking performance by electro-hydraulic ABS and motor torque control for in-wheel electric vehicle, *World Electric Vehicle Journal*, **6**(1): 186–191, 2013, https://doi.org/10.3390/wevj6010186.

18. Ji F., Tian M., Research on braking stability of electro-mechanical hybrid braking system in electric vehicles, *World Electric Vehicle Journal*, **4**(1): 217–223, 2010, https://doi.org/10.3390/wevj4010217.

19. Kovalchuk S., Goryk O., Burlaka O., Kelemesh A., Evaluation of the strength of the truck tractor's frame under emergency braking conditions, *The Archives of Automotive Engineering – Archiwum Motoryzacji*, **105**(3):74–87, 2024, https://doi.org/10.14669/AM/192345.

20. Akhmedov D., Riskaliev D., Modeling of full vehicle dynamics for enhanced stability control, *The Archives of Automotive Engineering – Archiwum Motoryzacji*, **105**(3): 88–102, 2024, https://doi.org/10.14669/AM/192666.

21. Esteem P.L., Ramalingam V.V., Kasi R.K., Ramasamy P., Development and tribological characterization of semi-metallic brake pads for automotive applications, *The Archives of Automotive Engineering – Archiwum Motoryzacji*, **102**(4): 5–25, 2023, https://doi.org/10.14669/AM/177327.

22. Simulink. Design. Simulate. Deploy, https://www.mathworks.com/products/simulink.html (retrieved on: 2024.10.26).

23. Toyota Yaris 2. Technical Data [in Polish], https://www.ultimatespecs.com/pl/samochody-dane-techniczne/Toyota/M361/Yaris-2 (retrieved on: 2024.10.26).

24. Tire-Road Interaction (Magic Formula), https://www.mathworks.com/help/physmod/sdl/ref/tireroadinteractionmagicformula.html (retrieved on: 2021.12.04).

25. Pacejka H.B., *Tire and Vehicle Dynamics*, Elsevier 2012.

26. Tadej M., Tadej M., Czech P, Gustof P., Hornik A., Jędrusik D., The impact of the ABS system on the achieved braking deceleration value of a passenger car [in Polish: Wpływ działania układu ABS na osiąg021 wartość opóźnienia hamowania samochodu osobowego], *Autobusy*, **17**(12): 447–453, 2016.